A Numerical Investigation of the Thermal Performance of a Double Pipe Heat Exchanger with Copper Foam Baffles

Zuhair S. Faal *‡, Abbas J. Jubear **, Hussain R. Al-Bugharbee ***

* Mechanical Engineering Department, Wasit University, Wasit, Iraq

(zuhairsa302@uowasit.edu.iq (Z. Sabah Rabeeah); abbasaljassani@uowasit.edu.iq (A.J. Jubear) ; hrazzaq@uowasit.edu.iq (H. R. Al-Bugharbee)

‡ Zuhair Sabah Faal Rabeeah , Tel: +009647705563031,

zuhairsa302@uowasit.edu.iq

Received: 09.11.2023 Accepted:15.01.2024

Abstract- Research on the enhancement of heat dissipation in heat exchangers using metallic foam still attracts the interest of the researchers' community. In the present study, the thermal performance of a double-pipe heat exchanger (DPHX) with a copper foam (CF) baffle inside is investigated numerically. Water is utilized as operating fluid in both pipes with parallel flow. Numerical simulation includes building the geometry to the heat exchanger and proposing the suitable dimensions, and open cell copper foam properties such as the pore density (PPI). This simulation examines the effect of metallic foam with porosity (0.9) on the heat exchanger performance. This is conducted by comparing different configurations of foam baffles inside the heat exchanger pipe. This includes a filled pipe heat exchanger with copper foam (HXFF) and partially baffles cases. In the partially filled cases, nine foam rings were proposed to be inserted inside the heat exchanger outer pipe. These rings are represented in different configurations including complete disks and rings with removed sectors of angle (β) oppositely. The angle (β) has two values 90° and 180°, the effect of pore density is also investigated by changing its value from 10 to 50PPI. The results explained that the heat transfer rate (Qave) and Nusselt number (Nuave) increase with increasing PPI and decrease of angle β. Enhancement in (Qave) and (Nuave) was (45%) and (146%) respectively in a heat exchanger at (β) (180°) with (40PPI). Similarly, the pressure drop (Δp) and the friction factor follow the same behavior, and the study included a comparison of the heat exchanger in the best configuration with (HXFF) and the heat exchanger without copper foam (HXOF).

Keywords Heat transfer enhancement, metal foam, performance evaluate criteria (PEC).

Nomenclature			
A_c	Cross section area of annular gap (m2)	Nu_s	Nusselt number without metal foam (smooth)
A_i, A_o	Inner and outer Surface area of inner pipe (m2)	P_r	Pyrantel Number
d_i, d_o	Inner and outer diameter of inner pipe (m)	p	Wetted perimeter (m)
D_i, D_o	Inner and outer diameter of outer pipe (m)	R_e	Renault Number
D_a	Darcy Number	T_f , T_s	Temperature of fluid and the solid matrix (ºK)
d_f	Fiber diameter (mm)	**Greek Symbols**	
d_p	Pore diameter (mm)	ρ	Density (kg/m3)
F	Inertial coefficient of metal foam	μ	Viscosity (N.S/m2)
k_{fe}	Effective thermal conductivity of fluid (W/m .k)	ε	Porosity of the porous medium
f_{MF}	Friction factor with metal foam	Δp	Pressure drop across the heat exchanger (Pa)
f_s	Friction factor without metal foam (smooth)	**Subscript**	
k_{se}	Effective thermal conductivity of solid (W/m .k)	i, o	Inlet and outlet

k_e	Effective thermal conductivity in metal foam (W/m .k)	h, c	Hot and cold
k	Permeability of the porous medium (m)	ave	Average
K	Thermal conductivity (W/m .k)	s	Surface
Nu_{MF}	Nusselt number with metal foam		

1. Introduction

According to the literature, using porous materials is considered one of the most important techniques for improving heat transfer in heat exchangers. Metal foams (MF) are one kind of porous material used in different heat exchangers including heat sinks as in [1-3]. As well as used in Electronics Cooling as in [4].

Chumpia & Hooman's 2014 [5], studied five sets of aluminum foam-wrapped tube heat exchangers MF with pore density (20PPI) and porosity (Ɛ) (0.901, 0.937) of varying thicknesses (5–20mm). Four tubes from aluminum and one from stainless steel. The results explained that the increased thickness of foam causes increasing the overall thermal resistance leading to decreasing the thermal efficiency and increasing the pressure drop. An experimental study was conducted by Arbak et al. 2017 [6], using 18 discs of open-cell aluminum foam with a thickness of 18.2mm and a porosity of 88.5% brazed to the inner surface of an aluminum pipe. where compared to a previous investigation using 20PPI. It was found that the maximum heat transfer is carried out at 40PPI while the lowest heat transfer is achieved at 20PPI. A micro-channel is the subject of numerical research by Alibeigi & Farahani, 2020 [7], that involves injecting fluid through its lower wall. The results explained that the heat transfer increases with the increased thickness of the porous medium layer.

Hamzah & Nima, 2020 [8], examined experimentally the air flow through copper metal foam fins of 40PPI oriented at a 30° angle with the flow direction in a double-pipe heat exchanger. They claimed that a MF increased the pressure drop slightly. Arasteh, Salimpour, and Tavakoli 2020 [9], conducted a numerical analysis of the best distribution to a fixed volume of a MF partially positioned in both pipes of a double-pipe heat exchanger. Results showed that partially filled with evenly distributed partitioned MF improves greater value of heat transfer rate than completely filled. In Maid, Hilal, and Lafta 2020 [10] study, heat transfer in a double-pipe heat exchanger with and without porous material was numerically analyzed. Alumina beads are placed into the tubes' interior, exterior, and both. In comparison to the situation without the metal pad, the findings showed the greatest value of the effectiveness had porous media in both tubes, larger pressure drops, and a higher Nusselt number. Chen et al. 2020 [11], examine numerically the thermal performance of a double-pipe heat exchanger filled with a MF that has a porosity (Ɛ) of 0.8-0.95 and a pore density (5-30PPI). They claimed that low porosity and high pore density result in an increase in effectiveness and pressure decreases. Experimental testing was conducted by Farhan, Fadhil, and Ahmed 2021 [12], which evaluated the performance of a double-pipe heat exchanger with copper metal foam (15PPI) and porosity (0.95), partially/periodically filled between the two pipes. The outcomes demonstrated that the usage of a MF increased the convection heat transfer coefficient. Alhusseny, Turan, and Nasser's, 2017 study [13], utilized porous material in the form of isotropic, homogeneous metal foam with a porosity (≥ 0.89) in a double-pipe heat exchanger. Utilizing both active and passive methods, they found that efficiency improved, and pumping energy was conserved as compared to heat exchangers that were filled.

The overall heat transfer rate and the pressure drop through a shell-tube heat exchanger with six porous baffles are investigated numerically by Pourrahmani, and M. H. Mohammadi, 2020 [14]. Three measurements were made for the baffle cut (25, 35, and 50 percent), permeability (10, 9, 12, and 15 m2), and porosity (0.2, 0.5, and 0.8). The findings indicated that a modest percentage baffle cut (25%) might enhance heat transmission while minimizing pressure loss. Naqvi & Wang, 2021 [15], estimated and evaluated using three different types of shell-tube heat exchangers with helical, segmental, as well as clamping baffles under the change of porosity and radius. They claimed that the shell must be filled partially with porous materials rather than filling it.

To the best of the authors' abilities, the research offers a thorough examination of the usage of partially filled annuli, something that most earlier literature did not do, especially when it came to the use of cut-out baffles. The study examines the effects of using different baffle designs on the thermal and hydraulic performance of double-pipe heat exchangers and selected open cell copper foam to make that due to the better type in heat dissipated as Borakhade and Mahalle, 2018 [16]. In contrast to previous research, this study examined additional parameters such as the shape and characteristics of copper foam baffles, wherein the baffle angle varied as β = (0°,90°, and 180°), the pore density varied as (10-50PPI), as well as to varies the flow rate (2, 3, 4, 5, 6 lpm) to compare the heat exchangers with and without metal foam.

The remaining sections of the current study include starting with the problem formulation, then a description of the model design and simulation method in the metals and methods section. After that, the results were presented and discussed, and the last section was the conclusions.

2. Problem Formulation

Figure 1, depicts the geometry of the problem under consideration. a DPHX has an Inner copper pipe and an Isolated outer Stainless steel pipe have corresponding diameters of 2cm and 6cm and a length of 60.96cm. due to the lightweight and large surface area of copper foam, therefore it is used. Nine pieces of CF with 10mm thickness are placed as baffles with spaced evenly apart across the annular region. These baffles are set up using cut triangular pieces with

different baffle angles (β) (0°, 90°, and 180°) oppositely to give three heat exchangers (HXB0, HXB90, and HXB180) respectively. The full ring has a baffle angle of (0°), this design leads to increased mixing and turbulent fluid. the flow is assumed as parallel flow with flow rate (2-6 lpm), steady state, turbulent, three-dimensional with water temperature at Outer pipe (30°C) for Cold water inlet ($T_{c,i}$) and (75°C) for Hot water inlet ($T_{h,i}$) at Inner Pipe inlet. Metal foam has a porosity of (0.9), homogenous, isotropic, open cell, and its pore density ranges from 10 to 50PPI. For fluid and metal foam, the governing equations (1) - (7) are:

Mass conservation law [17].

$$\frac{\partial Vx}{\partial x}+\frac{\partial Vy}{\partial y}+\frac{\partial Vz}{\partial z}=0 \quad (1)$$

Momentums equation according to Navier-Stokes and Newton's second law equations [18]:

In X-direction

$$\frac{1}{\varepsilon^2}\left(V_x\frac{\partial V_x}{\partial x}+V_y\frac{\partial V_x}{\partial y}+V_z\frac{\partial V_x}{\partial z}\right)=-\frac{\partial p}{\partial x}+\frac{1}{\varepsilon\,Re}\left(\frac{\partial^2 V_x}{\partial x^2}+\frac{\partial^2 V_x}{\partial y^2}+\frac{\partial^2 V_x}{\partial z^2}\right)-\frac{1}{Da\,Re}V_x-\frac{F}{\sqrt{Da}}V_x\left|\vec{V}\right| \quad (2)$$

In Y-direction

$$\frac{1}{\varepsilon^2}\left(V_x\frac{\partial V_y}{\partial x}+V_y\frac{\partial V_y}{\partial y}+V_z\frac{\partial V_y}{\partial z}\right)=-\frac{\partial p}{\partial y}+\frac{1}{\varepsilon\,Re}\left(\frac{\partial^2 V_y}{\partial x^2}+\frac{\partial^2 V_y}{\partial y^2}+\frac{\partial^2 V_y}{\partial z^2}\right)-\frac{1}{Da\,Re}V_y-\frac{F}{\sqrt{Da}}V_y\left|\vec{V}\right| \quad (3)$$

In Z-direction

$$\frac{1}{\varepsilon^2}\left(V_x\frac{\partial V_z}{\partial x}+V_y\frac{\partial V_z}{\partial y}+V_z\frac{\partial V_z}{\partial z}\right)=-\frac{\partial p}{\partial z}+\frac{1}{\varepsilon\,Re}\left(\frac{\partial^2 V_z}{\partial x^2}+\frac{\partial^2 V_z}{\partial y^2}+\frac{\partial^2 V_z}{\partial z^2}\right)-\frac{1}{Da\,Re}V_z-\frac{F}{\sqrt{Da}}V_z\left|\vec{V}\right| \quad (4)$$

Energy equation of the fluid in the porous medium (LTNE) is:

$$\left(V_x\frac{\partial T_f}{\partial x}+V_y\frac{\partial T_f}{\partial y}+V_z\frac{\partial T_f}{\partial z}\right)=\frac{(1+k_f)}{Pr\,Re}\left(\frac{\partial^2 T_f}{\partial y^2}+\frac{\partial^2 T_f}{\partial z^2}\right)+\frac{h_{sf}a_{sf}}{K_{sf}\,Pr\,Re}\left(T_s-T_f\right) \quad (5)$$

Energy equation of the solid matrix (LTNE):

$$0=\frac{\partial^2 T_s}{\partial y^2}+\frac{\partial^2 T_s}{\partial z^2}+\frac{h_{sf}a_{sf}}{K_{se}}\left(T_f-T_s\right) \quad (6)$$

Energy equation for an incompressible fluid (without foam):

$$(u.\nabla)T=\alpha\nabla.(\nabla T) \quad (7)$$

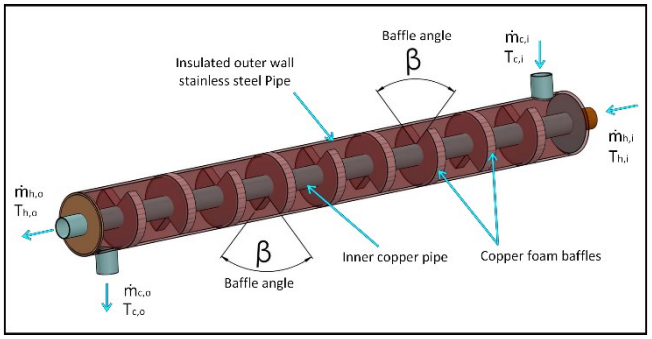

Fig. 1. Geometry of double pipe heat exchanger.

3. Materials and Methods

3.1. Numerical Calculations

By using a finite volume method to calculate heat transfer rates in steady state, three dimensions, and turbulent flow in complex geometric designs, CFD ANSYS FLUENT is suitable for that. The model-building functionality was given by Solidworks2022, while the mesh and relevant boundary conditions as well as the simulation of the current case's governing equations were provided by ANSYS 2020 R2.

3.1.1. Meshing Geometry

To choose the best mesh, a grid-independent test was conducted and the optimum number of elements was 4,600,000 elements. an acceptable mesh is used, Tetrahedron, Hexahedron, and inflation mesh technology. When comparing solutions by average Nusselt number for different mesh models, the resolution and accuracy must be taken into consideration as shown in Figure 2.

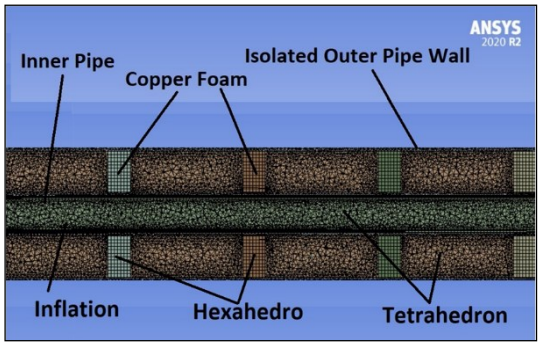

(a) Grid generated for present model.

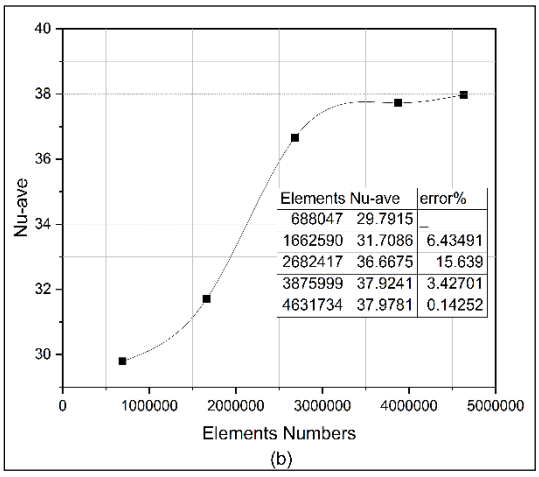

(b) Mesh independency.

Fig. 2. Meshing the geometry.

3.1.2. Setting Boundary Conditions

For a MF, a local thermal non-equilibrium (LTNE) model was taken into account. Water was employed as the working fluid. The momentum equation in a MF is explained by the Bringman-Forchheimer Darcy model, and the boundary conditions are explained in Table 1. Thus, The velocities coefficients represented by viscous resistance, which is the inverse of permeability, and the inertial loss coefficient must be defined and the interfacial surface (asf) area which

calculates in equations (8) - (12) and interfacial heat transfer coefficient (h_{sf}) was specified from User Define File (UDF) as a variable function with velocity [19], where: (ANSYS FLUENT User's Guide).

$$k = 0.00073\, dp^2(1-\varepsilon)^{-0.224}\left[\frac{d_f}{d_p}\right]^{-1.11} \tag{8}$$

$$F = 0.00212\,(1-\varepsilon)^{-0.132}\left[\frac{d_f}{d_p}\right]^{-1.36} \tag{9}$$

$$a_{sf} = \frac{3\pi d_f}{\left(0.59 d_p\right)^2}\left[1 - e^{-(1-\varepsilon)/0.04}\right] \tag{10}$$

$$\text{Viscous resistance} = \frac{1}{k} \tag{11}$$

$$\text{Inertial resistance} = \frac{2F}{k^2} \tag{12}$$

Table 1. The boundary conditions

Zone	Type	Momentum B.C.	Thermal B.C
cold-inlet	mass-flow-inlet	- Gage Pressure=0 Pa. - Reference: Absolute - Method: Normal to Boundary	Temperature
hot-inlet	mass-flow-inlet	- Gage Pressure=0 Pa. - Reference: Absolute - Method: Normal to Boundary	Temperature
cold-outlet hot-outlet	outflow	-	-
wall-outer-pipe	wall	Stationary, No slip	Insulated No heat flux
wall-inner-pipe	wall	Stationary, No slip	via system coupling

3.2. Mathematical Calculations

To complete the mathematical representation of the physical problem some the partial differential equations (13) - (27) must be solved.

3.2.1. Calculations of Thermal Performance

The heat transfer rate calculations are calculated as following procedure [20]:

Hot water heat transfer (Q_h)is:

$$Q_h = \left(\dot{m}C_p\right)_h\left(T_{h,i} - T_{h,o}\right) \quad \text{(W)} \tag{13}$$

Cold water heat transfer (Q_c) is:

$$Q_c = \left(\dot{m}C_p\right)_c\left(T_{c,o} - T_{c,i}\right) \quad \text{(W)} \tag{14}$$

The average heat transfer rate (Q_{ave}) is:

$$Q_{ave} = \frac{Q_h + Q_c}{2} \quad \text{(W)} \tag{15}$$

The maximum heat transfer (Q_{max}) is :

$$Q_{max} = \left(\dot{m}C_p\right)_h\left(T_{h,i} - T_{c,i}\right) \quad \text{(W)} \tag{16}$$

The effectiveness (E) of the double-pipe heat exchanger is :

$$E = \frac{Q_{ave}}{Q_{max}} \tag{17}$$

The convection heat transfer coefficient (h_i) between the hot water and the inner surface of the copper pipe:

$$h_i = \frac{Q_{ave}}{A_i(T_{h,ave} - T_{s,ave})} \quad \text{(W/m}^2\text{.°C)} \tag{18}$$

The log mean temperature difference (ΔT_{LM}) for parallel flow is:

$$\Delta T_{LM} = \frac{(T_{h.i} - T_{c.i}) - (T_{h.o} - T_{c.o})}{ln[(T_{h.i} - T_{c.i})/(T_{h.o} - T_{c.o})]} \quad \text{(°C)} \tag{19}$$

The overall heat transfer coefficient (U_i) is:

$$U_i = \frac{Q_{ave}}{A_i \Delta T_{LM}} \quad \text{(W/m}^2\text{.°C)} \tag{20}$$

The outer convection heat transfer coefficient of cold water (h_o) is:

$$h_o = \frac{1}{A_o\left(\frac{1}{U_i A_i} - \frac{1}{h_i A_i} - \frac{\ln\left(\frac{d_o}{d_i}\right)}{2\pi KL}\right)} \quad \text{(W/m}^2\text{.°C)} \tag{21}$$

The hydraulic diameter (D_h):

$$D_h = \frac{4A_c}{p}, \qquad A_c = \left(\frac{\pi}{4}\right)(D_i^2 - d_o^2) \tag{22}$$

$$D_h = \frac{4A_c}{p} = \frac{4 \times \left(\frac{\pi}{4}\right)(D_i^2 - d_o^2)}{\pi D_i + \pi d_o} = D_i - d_o \quad \text{(m)} \tag{23}$$

Where p: Wetted perimeter (m)

The average Nussle number (Nu_{ave}) annular pipe is :

$$Nu_{ave} = \frac{h_o D_h}{K_f} \tag{24}$$

3.2.2. Calculations of Hydraulic Performance

The velocity (u) was estimated using the following equation [8]:

$$u = \frac{\dot{V}}{A_c} = \frac{4\dot{V}}{\pi(D_i^2 - d_o^2)} \quad \text{(m/s)} \tag{25}$$

The friction factor (f) to stream at annular pipe is:

$$f = \frac{\Delta P(\frac{D_h}{L})}{\frac{\rho u^2}{2}} \tag{26}$$

Where ΔP : Pressure drop (pa)

3.2.3. Calculations of Performance Evaluate Criteria (PEC)

A (PEC) of the double-pipe heat exchanger is:

$$PEC = \frac{(\frac{Nu_{MF}}{Nu_s})}{(\frac{f_{MF}}{f_s})^{\frac{1}{3}}} \tag{27}$$

4. Results and Discussions

4.1. Validation

In order to determine the accuracy of the simulation software (Ansys2020 R2), it is necessary to validate the experimental model for a smooth double pipe heat exchanger before taking its dimensions to create a 3D drawing of the double-pipe heat exchanger by adding a MF that is utilized in the current study, E. Ebieto, R. Ana, E. Nyong, and G. Saturday, 2020 [21], was chosen to this validation, water flow rate (2, 3, and 4 lpm) in parallel and the temperature was changed over the heat exchanger, and as it was a laboratory model for university students as explained in Figure 3, the resulting deviations were (2.3%, 2%, and 1.8%).

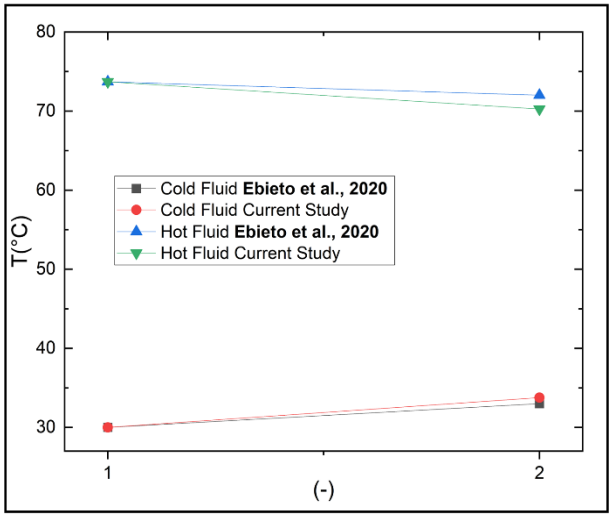

(a) Flow rate 2 lpm.

4.2. Numerical Results

Results are obtained and illustrated for the effect of pore density (PPI) and baffle angle (β) on the heat exchanger thermal performance at flow rate (2 lpm). The results include heat transfer rate (Q_{ave}), Nusselt number (Nu_{ave}), and the effectiveness (E). In addition, the hydraulic performance results in terms of the friction factor (f) and pressure drop (Δp) are also obtained. All the results above as well as the performance evaluate criteria (PEC) are shown for four heat exchangers with copper foam namely (HXFF, HXB0, HXB90, and HXB180).

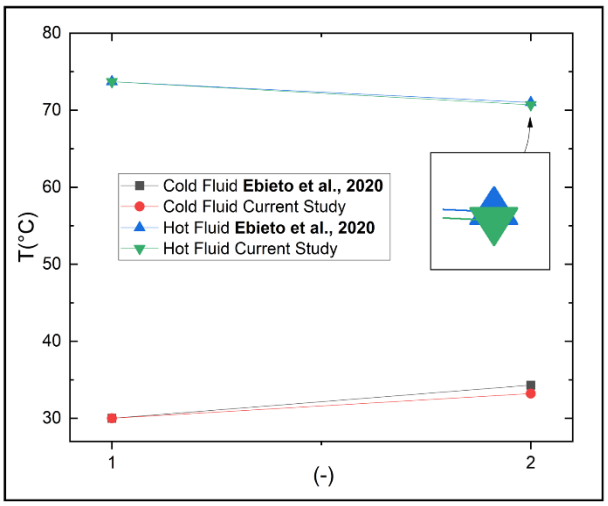

(b) Flow rate 3 lpm.

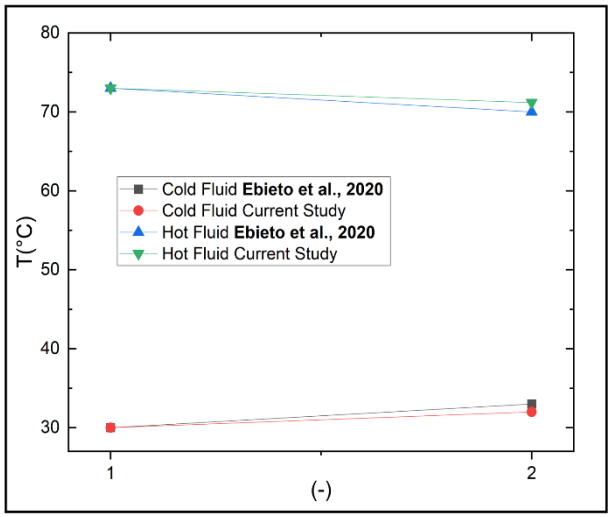

(c) Flow rate 4 lpm.

Fig. 3. Validation of Ebieto et al. 2020 [21].

4.2.1. Thermal Performance

Figure 4, depicts the effect of changing the PPI on the heat transfer rate (Q_{ave}), Nusselt number (Nu_{ave}), and the effectiveness (E). In this figure, the PPI changes from 10 to 50 with 10 step increment. It is clearly seen from Figure 3a. that the (Q_{ave}) increases with the increase of PPI in general. However, the (Q_{ave}) remains relatively stable when the PPI is 40 and above. A similar behavior can be noticed for the (Nu_{ave} and E)as in Figures 3b and 3c. The enhancement in (Q_{ave}, Nu_{ave}, and E) with the increase of PPI can be attributed to the increase of a MF surface area with increasing in porous density. The influence of copper foam volume by change (β) is also illustrated in the same figure, the parameters (Q_{ave}, Nu_{ave} and E) decrease with an increases (β), because decreased surface area of (CF). this decrease was gradually due to more mixing and turbulent flow grown with increase (β) which decreases the boundary layers.

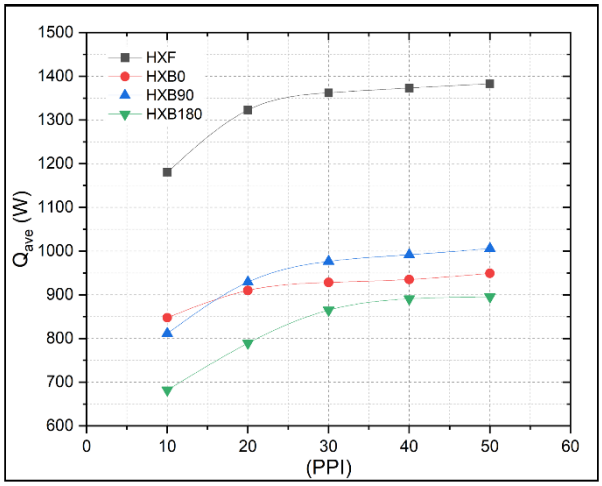

(a) Effect pore density and baffles angle on heat transfer.

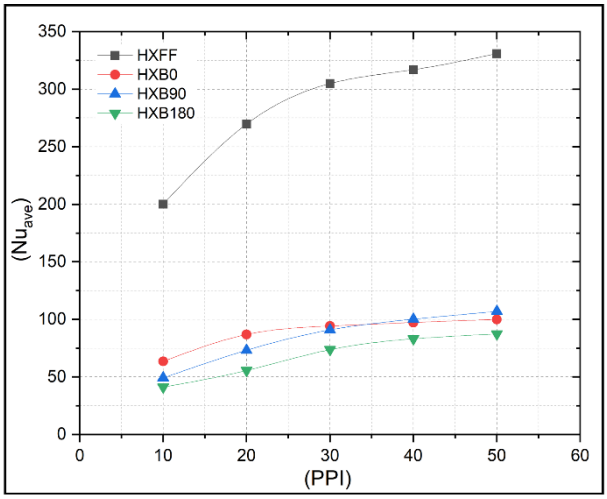

(b) Effect pore density and baffles angle on Nusselt number.

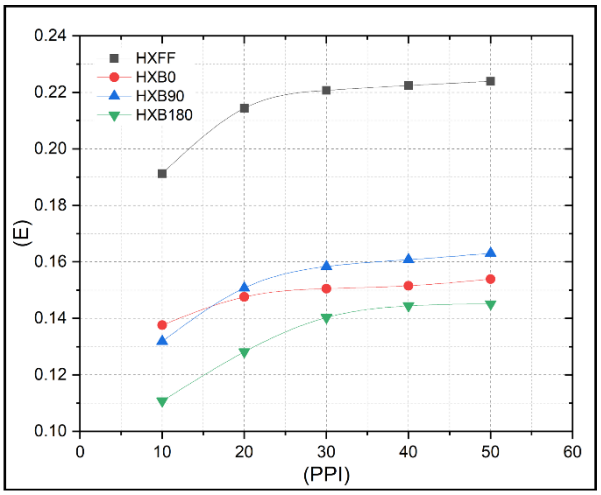

(c) Effect pore density and baffles angle on effectiveness.

Fig. 4. Effect of parameters (PPI, β) on thermal performance.

4.2.2. Hydraulic Performance

Figure 5, depicts the effect of changing PPI and baffles angle (β) on the hydraulic performance in terms of the pressure drop (Δp) and the friction factor (f) for all the heat exchanger models. The pressure drop becomes greater with the PPI growth. Similarly, the friction factor also increases when the PPI increases. In addition, it can be seen that the influence of PPI is significant in the case of HXFF and HXB0 models. This can be attributed to the restriction of water flow due to the obstruction made by foam materials.

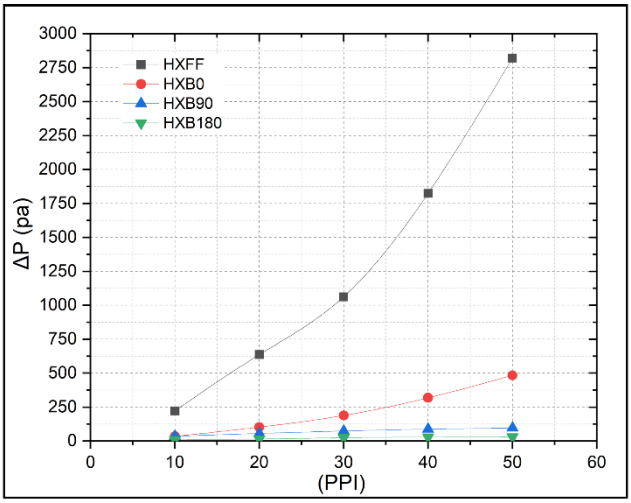

(a) Effect pore density and baffles angle on Pressure drop.

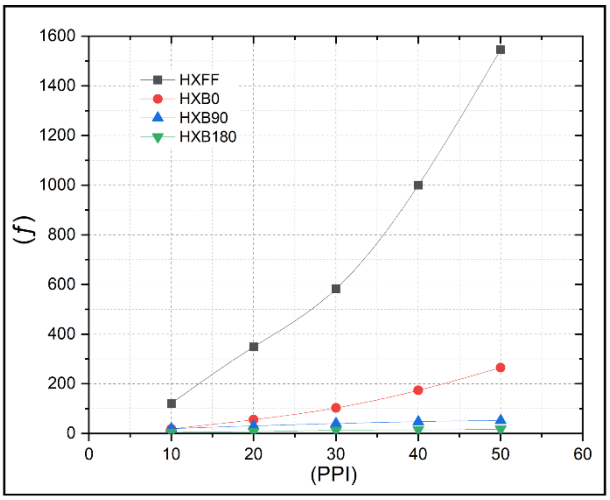

(b) Effect pore density and baffles angle on friction factor.

Fig. 5. Effect of parameters (PPI, β) on hydraulic performance.

4.2.3. Performance Evaluate Criteria (PEC)

As it was shown in the previous section the increase in PPI increases the thermal performance of the heat exchanger while it increases the (Δp) and (f). Thus, the overall influence of the heat exchanger performance can be made by computing the performance evaluation criteria (PEC) for all the heat exchanger models and under the variation of PPI. Figure 6, shows that the PEC of HXFF and HXB0 models dramatically decreases when Pore density becomes greater. On the other hand, the PEC of HXB90 and HXB180 models significantly increases with the increase of PPI. This indicates that PEC can be improved by reducing volume and raising Pore density.

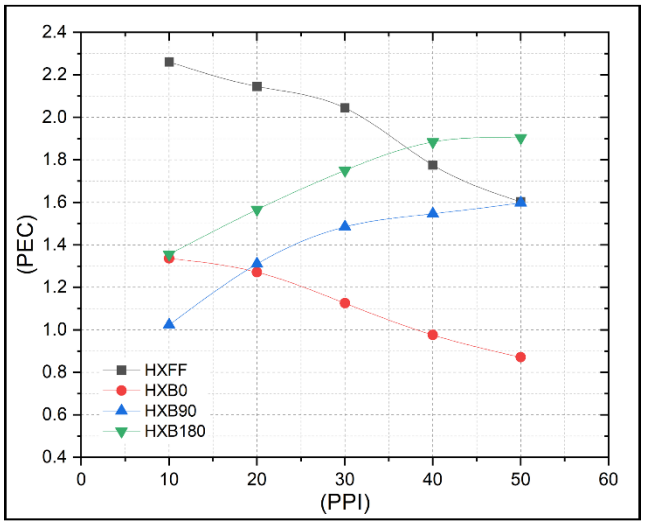

Fig. 6. Effect of parameters (PPI, β) on performance evaluate criteria (PEC).

4.3. Comparison of Contours Shapes

Comparisons were made between the performance evaluation criteria (PEC) of three different types of heat exchangers: HXOF, HXFF, and HXB180. The flow rate ranges between (2-6 lpm), and the comparable values are achieved at 40PPI. Figure 7 shows that a HXB180 with a PEC that was (72.7%) higher than a HXWFF was given the greatest average. The reason for this is that, even though the heat transfer rate between a HXFF and a HXOF is larger than the difference between a HXB180 and a HXOF by 63% and The Nusselt number and effectiveness were 241.5 and 64.6% respectively, the penalty for increasing the pressure drop and friction factor was very large in a HXFF.

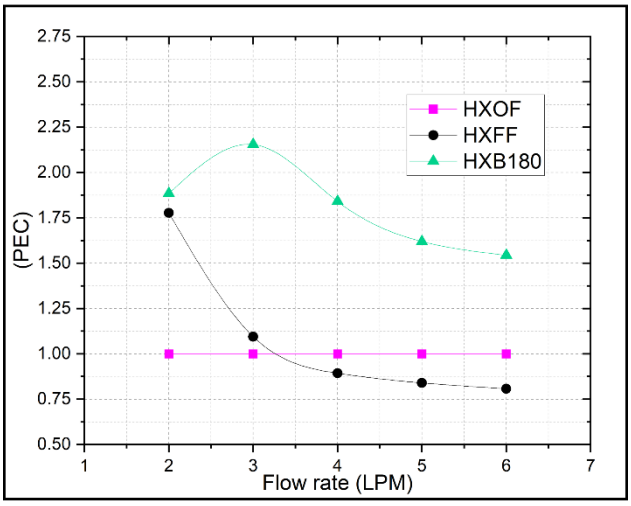

Fig. 7. Comparison of the effect of baffle angle (β) on performance evaluate criteria (PEC).

4.4. Comparison of Contours Shapes

Figure 8 compares contour forms from three heat exchangers (HXOF, HXFF, and HXB180) in a plane (X=58.8cm), explaining a side section at the fluid outlet and a front section portion in Figure 9. The bluish color was shown to be highest in a HXOF, to drop in a HXB180, and to be least focused in a HXFF. This indicates that the HXF has the most heat transfer convection. Furthermore, the reddish color of hot fluid at the inner pipe was the strongest in a HXOF and the weakest in a HXFF.

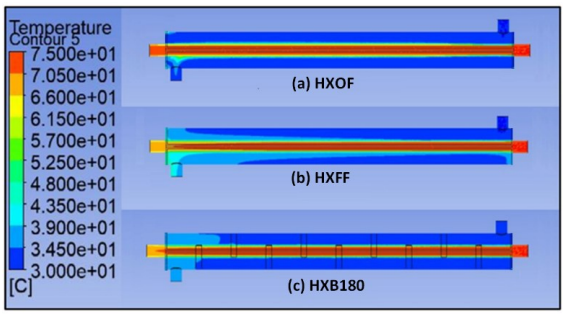

Fig. 8. Comparison of fluid temperature contours shapes (front section).

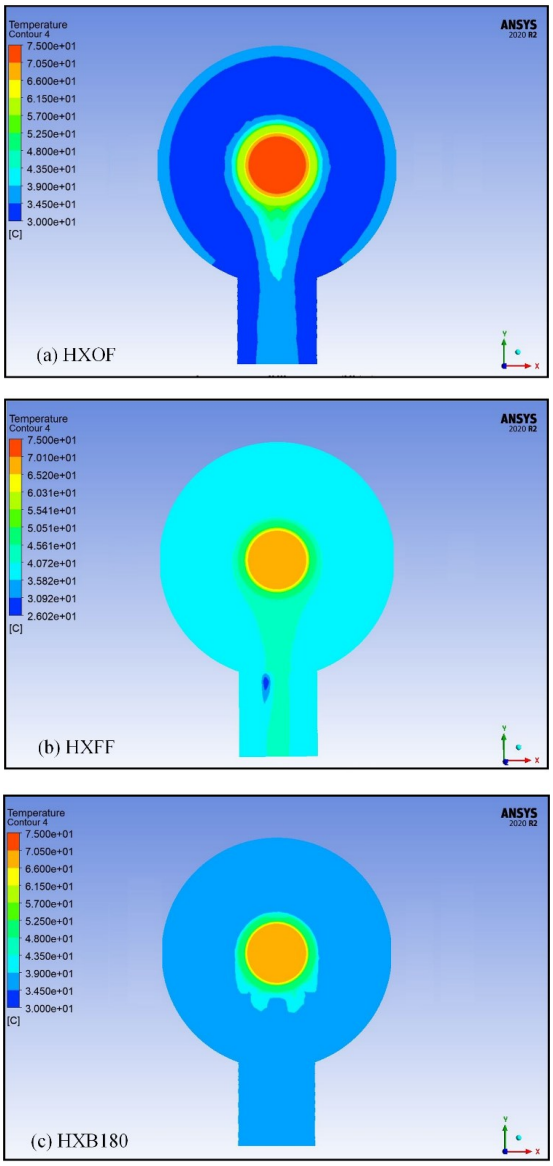

Fig. 9. Comparison of fluid temperature contours shapes (side section).

5. Conclusions

The effects of metal foam volume and pore density (PPI) in a double-pipe heat exchanger have been studied numerically. Four heat exchanger models containing a filled pipe heat exchanger with foam (HXFF) and three partially filled heat exchangers are used in the analysis. The partially filled models heat exchangers were with nine rings of foam baffles of 10mm thickness with various baffle angles (β) (0°, 90°, and 180°). The main findings made in the present study as presented below:

- Increasing the pore density of copper foam will improve all heat exchangers' thermal performance and increase pressure drop.
- Increasing the baffles angle (β) at pore density (10PP) results in reducing both thermal performance and both the (Δp) and (*f*).
- When the volume of foam is reduced and the pore density is increased after 10PPI, the rate of rise in the (Δp) and (*f*) is greater than the rate of increase in thermal performance, which results in reduction in the performance evaluate criteria (PEC) for (HXFF and HXB0) because they have a larger volume. And (HXB90 and HXB180) also will be increased in (PEC) because of their smaller volume. Where (PEC=1.88) for HXB180 at flow rate 2 lpm.
- A heat exchanger with partially full of metal foam is better than fully foam.
- A heat transfer rate (Q_{ave}) was (45%), where it was (615W) in a smooth pipe heat exchanger, while it was (895W) in HXB180 at flow rate 2 lpm.
- Nusselt number improvement (Nu_{ave}) was (146%), where it was (34) in a smooth pipe heat exchanger while it was (67) in HXB180 at flow rate 2 lpm.
- During the comparison of the three heat exchangers (HXOF, HXFF, and HXB180), it was discovered that the highest rate of PEC was for the exchanger (HXB180), and this is due to the penalty caused by the increase in the pressure drop of the exchanger (HXFF), even though it gives the highest of heat transfer rate.

References

[1] A. Radmanesh, N. Dukhan, M. Liang, and J. Engels, "Optimization of Metal Foam Heat Sinks for Electronic Air Cooling: Part I: Porosity," in 2023 22nd IEEE Intersociety Conference on Thermal and Thermomechanical Phenomena in Electronic Systems (ITherm), 2023, pp. 1–5. doi: 10.1109/ITherm55368.2023.10177660.

[2] H. Y. Zhang, C. Li, and P. Q. Fan, "Thermal and flow characteristics of device integrated metallic foam heat sinks with central impingement flow," in 2016 17th International Conference on Electronic Packaging Technology (ICEPT), 2016, pp. 477–481. doi: 10.1109/ICEPT.2016.7583179.

[3] A. Kovalevsky, A. Mats, M. Shmurak, and A. Fleisher, "Experimental Study of Aluminum Foams Thermal Conductivity. Prospects of Additive Manufacturing for Novel Heat Exchangers Production," in 2020 IEEE 10th International Conference Nanomaterials: Applications & Properties (NAP), 2020, pp. 02SAMA06-1-02SAMA06-6. doi: 10.1109/NAP51477.2020.9309706.

[4] J. Glass, Y. Avenas, D. Bouvard, and S. Ferrouillat, "An Analytical Model for the Optimisation of Metal Foam for Power Electronics Cooling," in 2019 25th International Workshop on Thermal Investigations of ICs and Systems (THERMINIC), 2019, pp. 1–6. doi: 10.1109/THERMINIC.2019.8923663.

[5] A. Chumpia and K. Hooman, "Performance evaluation of single tubular aluminium foam heat exchangers," Applied Thermal Engineering, vol. 66, no. 1–2, pp. 266–273, 2014, doi: https://doi.org/10.1016/j.applthermaleng.2014.01.071.

[6] A. Arbak, N. Dukhan, Ö. Bağcı, and M. Özdemir, "Influence of pore density on thermal development in open-cell metal foam," Experimental Thermal and Fluid Science, vol. 86, pp. 180–188, 2017, doi: https://doi.org/10.1016/j.expthermflusci.2017.04.012.

[7] M. Alibeigi and S. D. Farahani, "Effect of porous medium positioning on heat transfer of micro-channel with jet," International Journal of Engineering, vol. 33, no. 10, pp. 2057–2064, 2020.

[8] J. A. Hamzah and M. A. Nima, "Experimental study of heat transfer enhancement in double-pipe heat exchanger integrated with metal foam fins," Arabian Journal for Science and Engineering, vol. 45, no. 7, pp. 5153–5167, 2020, doi: 10.1007/s13369-020-04371-3.

[9] H. Arasteh, M. R. Salimpour, and M. R. Tavakoli, "Optimal distribution of metal foam inserts in a double-pipe heat exchanger," International Journal of Numerical Methods for Heat & Fluid Flow, 2019, doi: https://doi.org/10.1108/HFF-04-2018-0162.

[10] I. W. Maid, K. H. Hilal, and N. S. Lafta, "Numerical analysis for enhancing transferred heat in porous counter flow heat exchanger," in IOP Conference Series: Materials Science and Engineering, 2020, vol. 745, no. 1, p. 12081. doi: 10.1088/1757-899X/745/1/012081.

[11] X. Chen, X. Xia, C. Sun, F. Wang, and R. Liu, "Performance evaluation of a double-pipe heat exchanger with uniform and graded metal foams," Heat and Mass Transfer, vol. 56, no. 1, pp. 291–302, 2020, doi: https://doi.org/10.1007/s00231-019-02700-3.

[12] T. H. Farhan, O. T. Fadhil, and H. E. Ahmed, "Performance of a double-pipe heat exchanger with different met-al foam arrangements," Anbar Journal for Engineering Sciences, vol. 9, no. 2, pp. 100–112, 2021, doi: 10.37649/AENGS.2021.171162.

[13] A. Alhusseny, A. Turan, and A. Nasser, "Rotating metal foam structures for performance enhancement of double-pipe heat exchangers," International Journal of Heat and

Mass Transfer, vol. 105, pp. 124–139, 2017, doi: https://doi.org/10.1016/j.ijheatmasstransfer.2016.09.055

[14] H. R. Abbasi, E. S. Sedeh, H. Pourrahmani, M. H. Mohammadi, "Shape optimization of segmental porous baffles for enhanced thermo-hydraulic performance of shell-and-tube heat exchanger," Applied Thermal Engineering, vol. 180, p. 115835, 2020.

[15] S. M. A. Naqvi and Q. Wang, "Performance Enhancement of Shell–Tube Heat Exchanger by Clamping Anti-Vibration Baffles with Porous Media Involvement," Heat Transfer Engineering, vol. 42, no. 18, pp. 1523–1538, 2021, doi: https://doi.org/10.1080/01457632.2020.1807098.

[16] K. Borakhade and A. Mahalle, "Enhanced forced convection heat dissipation in power electronics systems by copper metal foam," in 2018 IEEE 8th Power India International Conference (PIICON), 2018, pp. 1–5. doi: 10.1109/POWERI.2018.8704413.

[17] A. Niameh and M. Alhusseny, "Heat transfer enhancement using rotating porous media table of contents," no. May. University of Manchester, p. 233, 2016. doi: https://ethos.bl.uk/OrderDetails.do?uin=uk.bl.ethos.756810.

[18] H. Abdullah, A. J. Jubear, and H. R. Al-Bugharbee, "Numerical and experimental thermal performance of forced convection in metal foam heat sinks," International Journal of Mechanical Engineering, vol. 7, no. 1, pp. 974–5823, 2022.

[19] A. J. Jubear, "CFD Simulation of Air Flow through a Copper Foams Fin Heat Sink under Forced Convection," no. March, 2022.

[20] H. E. Ahmed, O. T. Fadhil, and T. H. Farhana, "Performance of a double-pipe heat exchanger with different metal foam arrangements," Anbar Journal of Engineering Sciences, vol. 12, no. 2, 2021, doi: 10.37649/AENGS.2021.171162.

[21] C. E. Ebieto, R. R. Ana, O. E. Nyong, and E. G. Saturday, "Design and Construction of a Double Pipe Heat Exchanger for Laboratory Application," European Journal of Engineering and Technology Research, vol. 5, no. 11, pp. 1301–1306, 2020, doi: 10.24018/ejeng.2020.5.11.1950.